

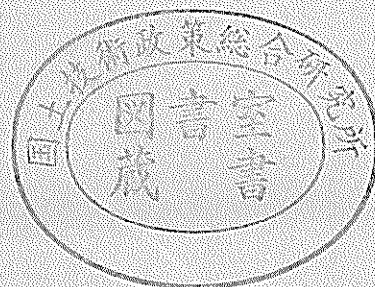
運輸省港湾技術研究所

港湾技術研究所 報告

REPORT OF
THE PORT AND HARBOUR RESEARCH
INSTITUTE
MINISTRY OF TRANSPORT

VOL. 27 NO. 3 SEPT. 1988

NAGASE, YOKOSUKA, JAPAN



港湾技術研究所報告 (REPORT OF P.H.R.I.)

第27巻 第3号 (Vol. 27, No. 3), 1988年9月 (Sept. 1988)

目 次 (CONTENTS)

1. Similitude for Shaking Table Tests on Soil-Structure-Fluid Model
in $1g$ Gravitational Field Susumu IAI 3
($1g$ 場での地盤—構造物—流体系の模型振動実験の相似則 井合 進)
2. Large Scale Model Tests and Analyses of Gravel Drains
..... Susumu IAI 25
(グラベルドレーンの大型模型振動実験と解析 井合 進)
3. 現地観測における水圧波形から表面波への換算手法について
..... 小舟浩治・合田良実・成田 明・佐々木 弘・森田行司... 161
(Surface Wave Recovery from Wave Pressures Profile Based on
Field Observation
..... Koji KOBUNE, Yoshimi GODA,
Akira NARITA, Hiroshi SASAKI and Yukiji MORITA)
4. 正規圧密地盤上の浅い基礎の支持力 北誥昌樹・遠藤敏雄・寺師昌明... 185
(Bearing Capacity of Shallow Foundation on Normally
Consolidated Ground
..... Masaki KITAZUME, Toshio ENDOH and Masaaki TERASHI)

1. Similitude for Shaking Table Tests on Soil-Structure-Fluid Model in 1 *g* Gravitational Field

Susumu IAI*

Synopsis

A similitude is derived for the shaking table tests on saturated soil-structure-fluid model in 1 *g* gravitational field. The main tool used for deriving the similitude is the basic equations which govern the equilibrium and the mass balance of soil skeleton, pore water, pile and sheet pile structures, and external waters such as sea. In addition to the basic equations, an assumption is made upon the constitutive law of soil; i.e. the stress-strain relation is determined irrespective of the confining pressures if appropriate scaling factors are introduced for the stress and the strain for taking the effect of the confining pressures into account.

Applicability of this assumption is examined by using the presently available data under the confining pressures ranging from 0.05 to 1 kgf/cm² (from 5 to 98 kN/m²) or 0.05 to 4 kgf/cm² (from 5 to 392 kN/m²). The results indicate that the assumption is applicable within the intermediate strain levels; i.e. the strain levels which are lower than the strains at failure. In consequence, the similitude derived in the present study is applicable to the model tests in which the major concern is directed toward the deformation, rather than the ultimate state of stability, of the soil-structure-fluid system.

Key Words: Deformation, Dynamic, Earthquake, Earthquake Resistant, Foundation Engineering [General], Liquefaction, Model Test

* Senior Research Engineer, Structural Engineering Division

1. $1g$ 場での地盤—構造物—流体系の 模型振動実験の相似則

井合 進*

要 旨

本研究では、 $1g$ 場での地盤—構造物—流体系の模型振動実験の相似則を求めた。相似則を求めるための方法には幾つかの方法があるが、本研究では、飽和した土の骨格、間隙水、杭や矢板、海などの流体に関する釣合および収支バランスの方程式を用いた。さらに、土の応力—歪関係に対して次の様な仮定を設けた。すなわち、土の応力—歪関係は、拘束圧力の影響を考慮するための適当な縮尺を応力と歪に導入すれば、拘束圧力に依存しない関係として定まる。この仮定を拘束圧力が 5-98 KPa ないし 5-392 KPa の範囲で実施された既往の試験データを用いて吟味した。その結果、この仮定は中程度の歪レベル、すなわち降伏時の歪未満の歪、において適用性を有することが分かった。このことから、本研究により求められた相似則は極限安定状態には適用できないが、変形を検討するための模型振動実験に対して幅広い適用性を有するとの結論を得た。

キーワード：液状化，基礎工学（一般），地震，耐震，動的，変形，模型実験

* 構造部主任研究官（地震動解析担当）

CONTENTS

Synopsis	3
1. Introduction	7
2. Basic Equations	7
2.1 Equations for Saturated Soil	8
2.2 Equations for Structures	9
3. Similitude	10
4. Applicability of Rocha's Assumptions.....	16
5. Applicability of the Similitude	19
6. Similitude Applied to Liquefaction	20
7. Conclusions.....	22
References	22
Notation	23

1. Introduction

Shaking table tests are often conducted in the $1g$ gravitational field in order to understand the behaviour of soil structures and foundations during earthquakes. On some occasions, the shaking table tests are conducted for the very complex models; the saturated soil-structure-fluid models under earthquake loadings. The necessity for such model tests is increasing nowadays because offshore and waterfront development is urgently requested in the seismically active areas in the world, especially in Japan.

In general, the similitude is necessary to interpret the results of the model tests. However, the similitude for the saturated soil-structure-fluid system is not clearly understood for the shaking table tests in the $1g$ gravitational field. There is a study on the similitude of soil structures under dynamic loadings by using the ratios of the forces (Kagawa, 1978). There is another study on the similitude of nonlinear dynamic responses of grounds by using Buckingham's π -theorem (Kokusho and Iwatate, 1979). Both of the studies resulted in the same similitude. However, the result of their studies is applicable only to the shear deformation of soil structures. There is a need to extend their similitude to a more general form in order to interpret the dynamic model tests of the saturated soil-structure-fluid system. In what follows, such a similitude will be shown by using basic equations which govern the dynamic behaviour of the saturated soil-structure-fluid system.

2. Basic Equations

Among the basic equations which govern the behaviour of saturated soil-structure-fluid system, the constitutive law of soil is one of the most important equations. Although the constitutive law of soil has been extensively studied as one of the main subjects in the soil mechanics, it is still under controversy. Therefore, in a strict sense, the basic equations on the behaviour of soil have not been fully

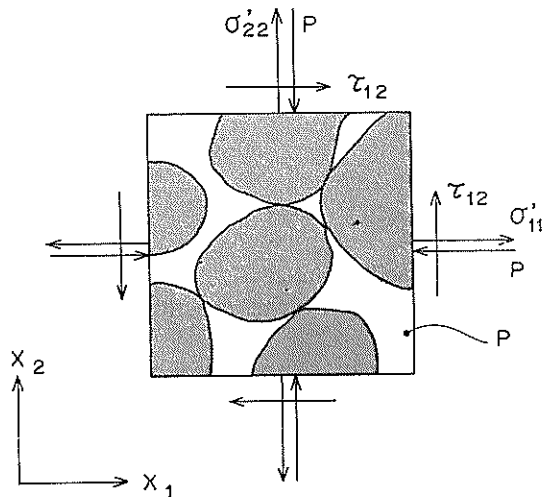


Fig. 1 Effective stress σ' of soil and pore water pressure p in an element of porous material

established. However, except for the constitutive law of soil, basic equations such as those for equilibrium and mass balance of soil skeleton, pore water, etc. have been well established for the dynamic behaviour of saturated soil-structure-fluid system as shown below.

2.1 Equations for Saturated Soil

First of all, let us regard the saturated soil as a porous material composed of two phases: a solid phase formed by the particles of soil and a liquid phase which fills the pore of the solid phase as shown in Fig. 1. The solid and the liquid phases will hereafter be called soil skeleton and pore water, respectively. Then, the behaviour of the saturated soil is governed by the following equations (Zienkiewicz et al., 1980):

Effective stress definition

$$\boldsymbol{\sigma} = \boldsymbol{\sigma}' - m\mathbf{p} \quad \dots\dots\dots(1)$$

Strain definition

$$d\boldsymbol{\varepsilon} = \mathbf{L}d\mathbf{u} \quad \dots\dots\dots(2)$$

Constitutive law

$$d\boldsymbol{\sigma} = \mathbf{D}(d\boldsymbol{\varepsilon} - d\boldsymbol{\varepsilon}^0 + mdp/3K_s) \quad \dots\dots\dots(3)$$

Overall equilibrium

$$\mathbf{L}^T\boldsymbol{\sigma} + \rho\mathbf{g} = \rho\ddot{\mathbf{u}} + \rho_f\ddot{\mathbf{w}} \quad \dots\dots\dots(4)$$

Equilibrium of pore water flow

$$-\nabla p + \rho_f\mathbf{g} = \mathbf{k}^{-1}\dot{\mathbf{w}} + \rho_f\ddot{\mathbf{u}} + \rho_f\ddot{\mathbf{w}} \quad \dots\dots\dots(5)$$

and

Mass balance

$$\nabla^T\mathbf{w} + \mathbf{m}^T\boldsymbol{\varepsilon} + pn/K_t + (1-n)p/K_s - \mathbf{m}^T\boldsymbol{\sigma}'/3K_s = 0 \quad \dots\dots\dots(6)$$

in which

$\boldsymbol{\sigma}^T = (\sigma_{11}, \sigma_{22}, \sigma_{33}, \tau_{12}, \tau_{23}, \tau_{31})$: total stress

$\boldsymbol{\sigma}'^T = (\sigma'_{11}, \sigma'_{22}, \sigma'_{33}, \tau'_{12}, \tau'_{23}, \tau'_{31})$: effective stress

$\mathbf{m}^T = (1, 1, 1, 0, 0, 0)$

p : pore water pressure

$\boldsymbol{\varepsilon}^T = (\varepsilon_{11}, \varepsilon_{22}, \varepsilon_{33}, \gamma_{12}, \gamma_{23}, \gamma_{31})$: strain

$$\mathbf{L}^T = \begin{bmatrix} \frac{\partial}{\partial x_1} & 0 & 0 & \frac{\partial}{\partial x_2} & 0 & \frac{\partial}{\partial x_3} \\ 0 & \frac{\partial}{\partial x_2} & 0 & \frac{\partial}{\partial x_1} & \frac{\partial}{\partial x_3} & 0 \\ 0 & 0 & \frac{\partial}{\partial x_3} & 0 & \frac{\partial}{\partial x_2} & \frac{\partial}{\partial x_1} \end{bmatrix}$$

$\mathbf{u}^T = (u_1, u_2, u_3)$: displacement of soil skeleton

\mathbf{D} : tangent modulus, which is defined by the constitutive law and generally depends on histories of $\boldsymbol{\sigma}'$, $\boldsymbol{\varepsilon}$, etc.

$\boldsymbol{\varepsilon}^0$: strain of soil skeleton due to creep, temperature, etc.

K_s : average bulk modulus of the solid grains forming the soil skeleton

\mathbf{g} : acceleration of gravity; $\mathbf{g}^T = (0, g, 0)$ ($g = 980\text{Gals}$) if the second component of the cartesian coordinates is taken pointing upward.

ρ : apparent density of two phase medium composed of soil and pore water; i. e. density of saturated soil

ρ_f : density of pore water

w^T : (w_1, w_2, w_3): Average displacement of pore water relative to the soil skeleton;
i. e. the ratio of the quantity of the pore water displaced over the total cross-sectional area

$$\nabla^T = \left(\frac{\partial}{\partial x_1}, \frac{\partial}{\partial x_2}, \frac{\partial}{\partial x_3} \right)$$

k : permeability

n : porosity of the soil skeleton

K_f : bulk modulus of the pore water

The boundary conditions are given by the following equations;

$$S\sigma = \bar{T} \quad \text{on } \Gamma_T \quad \dots\dots\dots(7)$$

$$u = \bar{u} \quad \text{on } \Gamma_u \quad \dots\dots\dots(8)$$

$$p = \bar{p} \quad \text{on } \Gamma_p \quad \dots\dots\dots(9)$$

$$w = \bar{w} \quad \text{on } \Gamma_w \quad \dots\dots\dots(10)$$

in which \bar{T} , \bar{u} , \bar{p} , \bar{w} are the traction force, displacement, pore water pressure, and relative displacement of pore water specified at each boundary, respectively, and S is a matrix which transforms the stress into the traction on the boundary Γ_T . Often the boundary value \bar{w} varies with time so that the value of \dot{w} i.e. the rate of flow of pore water, is specified on the boundary instead of w .

2.2 Equations for Structures

The structures usually constructed for offshore and waterfront development are idealised into either a solid (i.e. a figure which has three dimensions) or a beam (i.e. a figure which has one dimension). The equations for the solid are similar to those presented earlier if the variables of pore water are simply omitted from those equations. Therefore, the equations for the solid will not be explicitly written here. The equations for the beam are applicable both to the piles and sheet piles and are given as follows;

$$EI \frac{\partial^4 n^T u}{\partial n^4} + \rho_b n^T \ddot{u} - \rho_b n^T g + n^T S \sigma = 0 \quad \dots\dots\dots(11)$$

$$EA \frac{\partial^2 t^T u}{\partial s^2} + \rho_b t^T \ddot{u} - \rho_b t^T g + t^T S \sigma = 0 \quad \dots\dots\dots(12)$$

in which

EI : flexural rigidity (per unit breadth) = Young's modulus \times second moment of area (per unit breadth)

EA : longitudinal rigidity (per unit breadth) = Young's modulus \times cross sectional area (per unit breadth)

u : displacement of the beam

n : unit vector normal to the beam

t : unit vector tangential to the beam

$\frac{\partial}{\partial n}$: differentiation in the direction of n

$\frac{\partial}{\partial s}$: differentiation in the direction of t

ρ_b : density of the beam (mass per unit length and breadth)

S : a matrix which transforms the stress into the traction on the beam

σ : stress acting on the beam

Boundary conditions for the beam are given as follows;

$$\mathbf{u} = \bar{\mathbf{u}} \quad \text{at } \Gamma_{\bar{\mathbf{u}}} \quad \dots\dots\dots(13)$$

$$\frac{\partial \mathbf{n}^T \mathbf{u}}{\partial n} = \bar{\theta} \quad \text{at } \Gamma_{\bar{\theta}} \quad \dots\dots\dots(14)$$

$$EI \frac{\partial^2 \mathbf{n}^T \mathbf{u}}{\partial n^2} = \bar{M} \quad \text{at } \Gamma_{\bar{M}} \quad \dots\dots\dots(15)$$

$$EI \frac{\partial^3 \mathbf{n}^T \mathbf{u}}{\partial n^3} = \bar{S} \quad \text{at } \Gamma_{\bar{S}} \quad \dots\dots\dots(16)$$

$$EA \frac{\partial \mathbf{t}^T \mathbf{u}}{\partial s} = \bar{F} \quad \text{at } \Gamma_{\bar{F}} \quad \dots\dots\dots(17)$$

in which $\bar{\mathbf{u}}$, $\bar{\theta}$, \bar{M} , \bar{S} , and \bar{F} are the displacement, inclination, bending moment (per unit breadth), shear force (per unit breadth), and axial force (per unit breadth) specified at each boundary, respectively.

2.3 Equations for Fluid

The behaviour of the water such as sea during earthquakes can be approximated, by ignoring the viscosity of water and the wave generated by the motion of the structures, as follows (Lamb, 1932);

$$\nabla^2 p + \frac{\rho_f}{K_f} \ddot{p} = 0 \quad \dots\dots\dots(18)$$

in which

$$\nabla^2 = \frac{\partial^2}{\partial x_1^2} + \frac{\partial^2}{\partial x_2^2} + \frac{\partial^2}{\partial x_3^2}$$

- p: pressure of water
- ρ_f : density of water
- K_f : bulk modulus of water

At the boundaries between the structures and the water, the following equation is satisfied for the mass balance of water;

$$\frac{\partial p}{\partial n} = \rho_f \mathbf{n}^T \ddot{\mathbf{u}} \quad \dots\dots\dots(19)$$

in which

- \mathbf{n} : unit vector normal to the boundary between the structures and the water
- $\ddot{\mathbf{u}}$: acceleration at the boundary

Other boundary conditions are given by the following equations;

$$p = \bar{p} \quad \text{at } \Gamma_{\bar{p}} \quad \dots\dots\dots(20)$$

$$\frac{\partial p}{\partial n} = \bar{i} \quad \text{at } \Gamma_{\bar{i}} \quad \dots\dots\dots(21)$$

in which \bar{p} and \bar{i} are the pressure and the hydraulic gradient specified at each boundary.

3. Similitude

Let us denote the geometrical scale λ and the time scale λ_t ; namely,

$$(\mathbf{x})_p = \lambda (\mathbf{x})_m, (t)_p = \lambda_t (t)_m \quad \dots\dots\dots(22)$$

in which

$\mathbf{x}^T = (x_1, x_2, x_3)$: cartesian coordinate

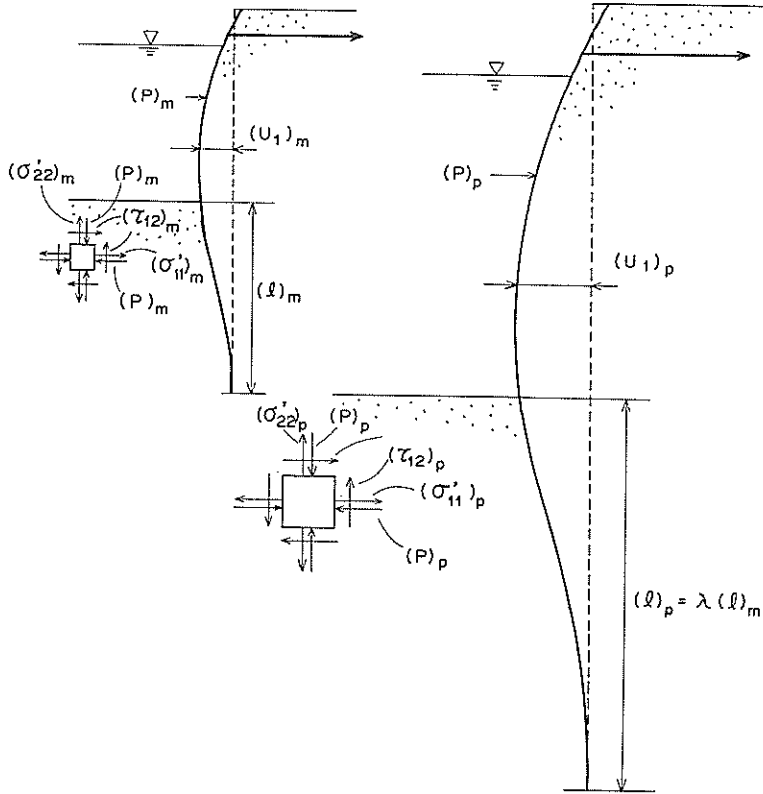


Fig. 2 Displacements u , effective stresses σ' and pressures of pore water and external water p in the model and the prototype

and subscripts m and p denote model and prototype, respectively.

Then, the following relationships are derived, between the model and the prototype. for the differential operators in the basic equations (1) through (21);

$$\begin{aligned}
 (\mathbf{L})_p &= \frac{1}{\lambda} (\mathbf{L})_m, \quad \left(\frac{\partial}{\partial n} \right)_p = \frac{1}{\lambda} \left(\frac{\partial}{\partial n} \right)_m, \quad (\nabla)_p = \frac{1}{\lambda} (\nabla)_m, \\
 \left(\frac{\partial}{\partial t} \right)_p &= \frac{1}{\lambda t} \left(\frac{\partial}{\partial t} \right)_m, \quad \text{etc.} \quad \dots\dots\dots(23)
 \end{aligned}$$

Let us assume the following relationships, between the model and the prototype such as shown in Fig. 2, for the variables and the coefficients in the equations (1) through (21);

$$\left. \begin{aligned}
 (\boldsymbol{\epsilon})_p &= \lambda_\epsilon (\boldsymbol{\epsilon})_m, \quad (\boldsymbol{\epsilon}^0)_p = \lambda_\epsilon^0 (\boldsymbol{\epsilon}^0)_m, \\
 (\boldsymbol{\sigma})_p &= \lambda_\sigma (\boldsymbol{\sigma})_m, \quad (\boldsymbol{\sigma}')_p = \lambda_{\sigma'} (\boldsymbol{\sigma}')_m, \\
 (\mathbf{D})_p &= \lambda_D (\mathbf{D})_m, \quad (\mathbf{K}_s)_p = \lambda_{K_s} (\mathbf{K}_s)_p, \\
 (p)_p &= \lambda_p (p)_m, \quad (\mathbf{k})_p = \lambda_k (\mathbf{k})_m, \\
 (\mathbf{u})_p &= \lambda_u (\mathbf{u})_m, \quad (\mathbf{w})_p = \lambda_w (\mathbf{w})_m, \\
 (\mathbf{n})_p &= \lambda_n (\mathbf{n})_m, \quad (\mathbf{K}_f)_p = \lambda_{K_f} (\mathbf{K}_f)_m, \\
 (\mathbf{EI})_p &= \lambda_{EI} (\mathbf{EI})_m, \quad (\mathbf{EA})_p = \lambda_{EA} (\mathbf{EA})_m, \\
 (\rho)_p &= \lambda_\rho (\rho)_m, \quad (\rho_f)_p = \lambda_{\rho_f} (\rho_f)_m, \quad (\rho_b)_p = \lambda_{\rho_b} (\rho_b)_m,
 \end{aligned} \right\} \dots\dots\dots(24)$$

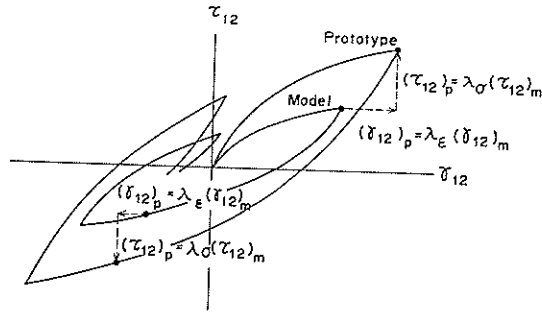


Fig. 3 Stress-strain relations of soils in the model and the prototype

$$\left. \begin{aligned} (\bar{T})_p &= \lambda_T (\bar{T})_m, (\bar{u})_p = \lambda_u (\bar{u})_m, (\bar{p})_p = \lambda_p (\bar{p})_m, (\bar{w})_p = \lambda_w (\bar{w})_m, \\ (\bar{\theta})_p &= \lambda_\theta (\bar{\theta})_m, (\bar{M})_p = \lambda_M (\bar{M})_m, (\bar{S})_p = \lambda_S (\bar{S})_m, (\bar{F})_p = \lambda_F (\bar{F})_m, \end{aligned} \right\}$$

Among these assumptions, the assumptions on the stress and the strain play a crucial role in deriving the similitude and may well be called Rocha's assumptions for paying homage to his pioneering work (Rocha, 1957). An illustrative example of Rocha's assumptions is shown in Fig. 3. Applicability of Rocha's assumptions will be discussed in the following chapter.

The similitude is derived as the conditions for the equations (1) through (21) being satisfied both in the model and the prototype. For example, let us regard Eq. (1) as the equation for the prototype as follow;

$$(\sigma)_p = (\sigma')_p - m(p)_p \tag{1'}$$

By substituting Eq. (24) into Eq. (1'), we can get

$$\lambda_\sigma (\sigma)_m = \lambda_{\sigma'} (\sigma')_m - \lambda_p m(p)_m \tag{1''}$$

In order to satisfy Eq. (1) in the model as well as in the prototype, the following equation should be satisfied;

$$(\sigma)_m = (\sigma')_m - m(p)_m \tag{1'''}$$

Comparison between Eqs. (1'') and (1''') gives

$$\lambda_\sigma = \lambda_{\sigma'} = \lambda_p \tag{25}$$

Similarly, the following conditions are derived from Eqs. (2) through (21);

From Eq. (2)

$$\lambda_\epsilon = \lambda_u / \lambda \tag{26}$$

From Eq. (3)

$$\lambda_{\sigma'} = \lambda_D \lambda_\epsilon = \lambda_D \lambda_\epsilon^0 = \lambda_D \lambda_p / \lambda_{K_s} \tag{27}$$

From Eq. (4)

$$\lambda_\sigma / \lambda = \lambda_p = \lambda_p \lambda_u / \lambda_\epsilon^2 = \lambda_{\rho t} \lambda_w / \lambda_\epsilon^2 \tag{28}$$

From Eq. (5)

$$\lambda_p / \lambda = \lambda_{\rho t} = \lambda_w / (\lambda_t \lambda_k) = \lambda_{\rho t} \lambda_u / \lambda_\epsilon^2 = \lambda_{\rho t} \lambda_w / \lambda_\epsilon^2 \tag{29}$$

From Eq. (6)

$$\lambda_w / \lambda = \lambda_\epsilon = \lambda_p \lambda_n / \lambda_{K_t} = \lambda_p / \lambda_{K_s} = \lambda_n \lambda_p / \lambda_{K_s} = \lambda_{\sigma'} / \lambda_{K_s} \tag{30}$$

From Eq. (7)

$$\lambda_\sigma = \lambda_T \tag{31}$$

Similitude for Shaking Table Tests on Soil-Structure-Fluid Model in 1 *g* Field

From Eq. (8)	$\lambda_u = \lambda_a$(32)
From Eq. (9)	$\lambda_p = \lambda_{\bar{p}}$(33)
From Eq. (10)	$\lambda_w = \lambda_{\bar{w}}$(34)
From Eq. (11)	$\lambda_{EI} \lambda_u / \lambda^4 = \lambda_{\rho_b} \lambda_u / \lambda t^2 = \lambda_{\rho_b} = \lambda_{\sigma}$(35)
From Eq. (12)	$\lambda_{EA} \lambda_u / \lambda^2 = \lambda_{\rho_b} \lambda_u / \lambda t^2 = \lambda_{\rho_b} = \lambda_{\sigma}$(36)
From Eq. (13)	$\lambda_b = \lambda_{\bar{b}}$(37)
From Eq. (14)	$\lambda_u / \lambda = \lambda_{\bar{v}}$(38)
From Eq. (15)	$\lambda_{EI} \lambda_u / \lambda^2 = \lambda_{\bar{M}}$(39)
From Eq. (16)	$\lambda_{EI} \lambda_u / \lambda^3 = \lambda_{\bar{S}}$(40)
From Eq. (17)	$\lambda_{EA} \lambda_u / \lambda = \lambda_{\bar{P}}$(41)
From Eq. (18)	$\lambda_{\rho} / \lambda^2 = \lambda_{\rho_t} \lambda_{\rho} / (\lambda \kappa_t \lambda t^2)$(42)
From Eq. (19)	$\lambda_{\rho} / \lambda = \lambda_{\rho_t} \lambda_u / \lambda t^2$(43)
From Eq. (20)	$\lambda_{\rho} = \lambda_{\bar{\rho}}$(44)
From Eq. (21)	$\lambda_{\rho} / \lambda = \lambda_i$(45)

Among Eqs. (25) through (45), there are apparently 37 equalities but number of the equalities which are independent from each other are only 25. For example, it is possible to identify that the following equalities are not independent from the rest of the equalities; the third and the fourth equalities in Eq. (29), the first, the third and the fifth equalities in Eq. (30), the second equality in Eq. (35), the second and the third equalities in Eq. (36), the equalities in Eqs. (37), (42), (43), and (44). On the other hand, number of the scaling factors appearing in Eqs. (25) through (45) are 28 as understood from Eqs. (22) and (24). Therefore, Eqs. (25) through (45) will be solved for three independent scaling factors. Let us regard the following scaling factors as the independent ones; the geometric scaling factor λ , the scaling factor for density of saturated soil λ_{ρ} , and the scaling factor for strain of saturated soil λ_{ϵ} . Then, from Eqs. (25) through (45), the similitude is obtained as shown in **Table 1**. In the special case in which $\lambda_{\rho} = 1$ and $\lambda_{\epsilon} = \lambda^{0.5}$, the similitude is reduced as shown in **Table 2**. In this case, the similitude for the soil skeleton becomes the same as that developed by Kagawa (1978) and Kokusho and Iwatate (1979).

In general λ_{ϵ} can be more accurately determined if the shear wave velocity of

Table 1 Similitude for model tests in 1g gravitational field

	Items	Scaling factors (prototype/model)
x	length	λ
ρ	density of saturated soil	λ_ρ
ϵ	strain of soil	λ_ϵ
t	time	$(\lambda\lambda_\epsilon)^{0.5}$
e^0	strain of soil due to creep, temperature, etc.	λ_ϵ
σ	total stress of soil	$\lambda\lambda_\rho$
σ'	effective stress of soil	$\lambda\lambda_\rho$
D	tangent modulus of soil, which generally depends on histories of effective stress, strain, etc.	$\lambda\lambda_\rho/\lambda_\epsilon$
K_s	bulk modulus of the solid grains of soil	$\lambda\lambda_\rho/\lambda_\epsilon$
p	pressure of pore water and/or external water	$\lambda\lambda_\rho$
k	permeability of soil	$(\lambda\lambda_\epsilon)^{0.5}/\lambda_\rho$
u	displacement of soil and/or structure	$\lambda\lambda_\epsilon$
\dot{u}	velocity of soil and/or structure	$(\lambda\lambda_\epsilon)^{0.5}$
\ddot{u}	acceleration of soil and/or structure	1
w	average displacement of pore water relative to the soil skeleton	$\lambda\lambda_\epsilon$
\dot{w}	rate of pore water flow	$(\lambda\lambda_\epsilon)^{0.5}$
n	porosity of soil	1
K_f	bulk modulus of pore water and/or external water	$\lambda\lambda_\rho/\lambda_\epsilon$
EI	flexural rigidity (per unit breadth of the beam)	$\lambda^4\lambda_\rho/\lambda_\epsilon$
EA	longitudinal rigidity (per unit breadth of the beam)	$\lambda^2\lambda_\rho/\lambda_\epsilon$
θ	inclination of the beam	λ_ϵ
M	bending moment of the beam (per unit breadth of the beam)	$\lambda^3\lambda_\rho$
S	shear force of the beam (per unit breadth of the beam)	$\lambda^2\lambda_\rho$
F	axial force of the beam (per unit breadth of the beam)	$\lambda^2\lambda_\rho$
ρ_f	density of pore water and/or external water	λ_ρ
ρ_b	density of the beam (mass per unit length and breadth of the beam)	$\lambda\lambda_\rho$
\bar{T}	traction acting on the soil specified on the boundary	$\lambda\lambda_\rho$
\bar{u}	displacement of the soil and/or the beam specified on the boundary	$\lambda\lambda_\epsilon$
\bar{w}	average displacement of pore water, specified on the boundary, relative to the soil skeleton, often specified as rate of flow on the boundary	$\lambda\lambda_\epsilon$
$\bar{\theta}$	inclination of the beam specified at the boundary	λ_ϵ
\bar{M}	bending moment of the beam specified at the boundary (per unit breadth of the beam)	$\lambda^3\lambda_\rho$
\bar{S}	shear force of the beam specified at the boundary (per unit breadth of the beam)	$\lambda^2\lambda_\rho$
\bar{F}	axial force of the beam specified at the boundary (per unit breadth of the beam)	$\lambda^2\lambda_\rho$
\bar{i}	hydraulic gradient of external water specified at the boundary	λ_ρ

Similitude for Shaking Table Tests on Soil-Structure-Fluid Model in 1g Field

Table 2 Similitude for model tests in 1g gravitational field in the special case in which $\lambda_\rho=1$ and $\lambda_\epsilon=\lambda^{0.5}$

Items		Scaling factors (prototype/model)
x	length	λ
ρ	density of saturated soil	1
ϵ	strain of soil	$\lambda^{0.5}$
t	time	$\lambda^{0.75}$
ϵ^0	strain of the soil due to creep, temperature, etc.	$\lambda^{0.5}$
σ	total stress of soil	λ
σ'	effective stress of soil	λ
D	tangent modulus of soil, which generally depends on histories of effective stress, strain, etc.	$\lambda^{0.5}$
K_s	bulk modulus of the solid grains of soil	$\lambda^{0.5}$
p	pressure of pore water and/or external water	λ
k	permeability of soil	$\lambda^{0.75}$
u	displacement of soil and/or structure	$\lambda^{1.5}$
\dot{u}	velocity of soil and/or structure	$\lambda^{0.75}$
\ddot{u}	acceleration of soil and/or structure	1
w	average displacement of pore water relative to the soil skeleton	$\lambda^{1.5}$
\dot{w}	rate of pore water flow	$\lambda^{0.75}$
n	porosity of soil	1
K_f	bulk modulus of pore water and/or external water	$\lambda^{0.5}$
EI	flexural rigidity (per unit breadth of the beam)	$\lambda^{3.5}$
EA	longitudinal rigidity (per unit breadth of the beam)	$\lambda^{1.5}$
θ	inclination of the beam	$\lambda^{0.5}$
M	bending moment of the beam (per unit breadth of the beam)	λ^3
S	shear force of the beam (per unit breadth of the beam)	λ^2
F	axial force of the beam (per unit breadth of the beam)	λ^2
ρ_f	density of pore water and/or external water	1
ρ_b	density of the beam (mass per unit length and breadth of the beam)	λ
\bar{T}	traction acting on the soil specified on the boundary	λ
\bar{u}	displacement of the soil and/or the beam specified on the boundary	$\lambda^{1.5}$
\bar{p}	pressure of pore water and/or external water on the boundary	λ
\bar{w}	average displacement of pore water, specified on the boundary, relative to the soil skeleton, often specified as rate of flow on the boundary	$\lambda^{1.5}$
$\bar{\theta}$	inclination of the beam specified at the boundary	$\lambda^{0.5}$
\bar{M}	bending moment of the beam specified at the boundary (per unit breadth of the beam)	λ^3
\bar{S}	shear force of the beam specified at the boundary (per unit breadth of the beam)	λ^2
\bar{F}	axial force of the beam specified at the boundary (per unit breadth of the beam)	λ^2
\bar{i}	hydraulic gradient of external water specified at the boundary	1

the model ground $(V_s)_m$ and that of the prototype ground $(V_s)_p$, are available. The shear moduli at the small strain level of the model ground $(G_o)_m$ and the prototype ground $(G_o)_p$ are determined as follows;

$$\left. \begin{aligned} (G_o)_m &= (\rho)_m (V_s)_m^2 \\ (G_o)_p &= (\rho)_p (V_s)_p^2 \end{aligned} \right\} \dots\dots\dots(46)$$

These moduli give the scaling factor for the tangent modulus of soil as

$$\begin{aligned} \lambda_D &= (\rho)_p (V_s)_p^2 / [(\rho)_m (V_s)_m^2] \\ &= \lambda_\rho [(V_s)_p / (V_s)_m]^2 \end{aligned} \dots\dots\dots(47)$$

whereas the similitude in Table 1 gives

$$\lambda_D = \lambda \lambda_\rho / \lambda_\epsilon \dots\dots\dots(48)$$

Consequently, the scaling factor for the strain is given by

$$\lambda_\epsilon = \lambda / [(V_s)_p / (V_s)_m]^2 \dots\dots\dots(49)$$

4. Applicability of Rocha's Assumptions

For deriving the similitude in this study, Eq. (24) was assumed. Obviously, most of the assumptions made in Eq. (24) can be understood as valid for deriving the similitude. However, the assumptions made for the stress and the strain, i.e. Rocha's assumptions, should be carefully evaluated because, as mentioned earlier, the constitutive law of the soil is still under controversy.

Recently, Tatsuoka et al. (1986) conducted plane strain compression tests under the confining pressures ranging from 0.05 to 4.0 kgf/cm² (from 5 to 392 kN/m²) and obtained the relations between the axial strain and the stress ratio σ'_1/σ'_3 and between the axial and the volumetric strains as shown in Fig. 4. This result seems to support the use of scaling factors in the stress and the strain for studying deformation of soils. If the value of σ'_3 is regarded as the scaling factor which is proportional to the confining pressure σ'_c , the compression stress σ'_1 is already normalised by the scaling factor σ'_3 in Fig. 4. If the axial strain in Fig. 4 is normalised with an

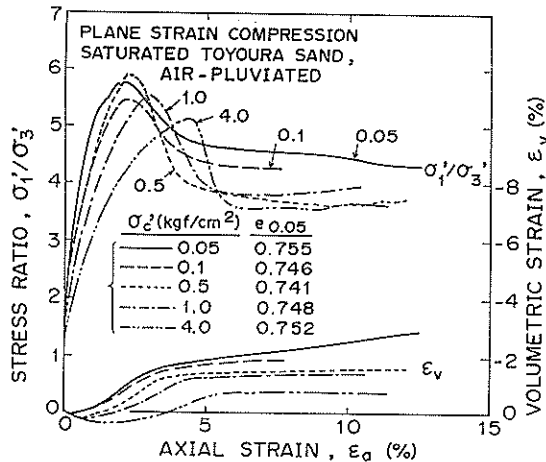


Fig. 4 Stress-strain relations of Toyoura sand at the confining pressures ranging from 0.05 to 4 kgf/cm² (from 5 to 392 kN/m²) (after Tatsuoka, et al, 1986)

appropriate scaling factor which takes the effect of confining pressures into account, the stress ratio seems to be uniquely determined by the normalised axial strain. Moreover, if the volumetric strain, as well as the axial strain, is normalised with the appropriate scaling factor, the normalised volumetric strain seems to be uniquely determined by the normalised axial strain. In short, Rocha's assumptions seem to be applicable to the test result in Fig. 4.

Obviously, the stress ratios and the volumetric strains at the range around or beyond the axial strains at the peak stress ratios in Fig. 4 cannot be uniquely determined even if a scaling factor is introduced in the axial strain. This may be one of the reasons why the similitude suggested by Rocha is not consistent with the findings on the scaling effect of ultimate bearing capacity of shallow foundation (de Beer, 1965; Yamaguchi et al., 1976). In the ultimate state of stability of soil structures and foundations, Casagrande's critical void ratio plays a major role. The critical void ratio depends on the confining pressures (Taylor, 1948). Therefore, Rocha's assumptions are not applicable to the ultimate state of stability of soil structures and foundations.

However, in the dynamic model tests, major concern is usually directed toward deformation, rather than the ultimate state of stability, of soil structures and foundations. When the saturated soil structures and foundations are shaken by strong earthquake motions, they will suffer some degree of residual deformations. If the degree of residual deformation is very large, the soil structures might well be considered having lost their stability against earthquakes. On the contrary, if the degree of residual deformation is very small, the soil structures might well be considered having kept their stability. There are many cases in which the degree of residual deformation is neither very large nor very small. Thus, in assessing the stability of soil structures and foundations against earthquake motions, it is very important to assess the degree of residual deformation.

The importance of assessing the degree of residual deformation against earthquake loadings stems from the specific nature of the behaviour of saturated sand under earthquake loadings; the undrained behaviour of the sand. If the effective stress state of soil skeleton becomes close to the failure, the effective confining

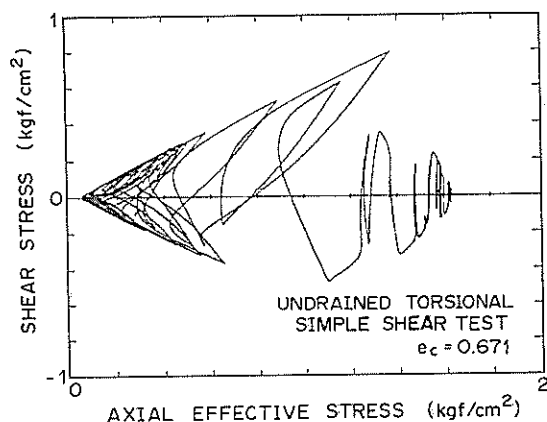


Fig. 5 Stress path of Toyoura sand under undrained torsional simple shear test (after Pradhan, et al, 1987)

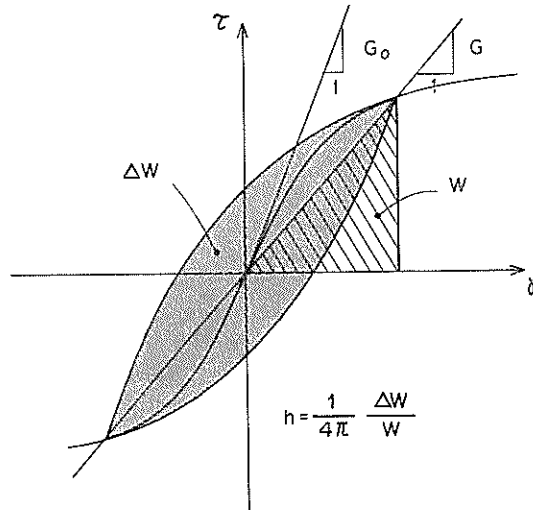


Fig. 6 Typical stress-strain relations under cyclic loadings, the secant shear modulus, and the hysteretic damping factor

pressure becomes large due to the dilatant nature of the soil skeleton except for the extremely loose sand. If the effective confining pressure becomes large, the shear strength becomes proportionally large. Therefore, it is difficult for the saturated sand to achieve the failure under earthquake loadings. An example of the effective stress path obtained at the undrained simple shear test under earthquake loadings is shown in Fig. 5 (after Pradhan, et al., 1987).

Consequently, the behaviour of saturated soil under earthquake loadings is generally governed by the behavior of soils within the limited range of strains which are smaller than the strains at failure. Thus, the test results shown in Fig. 4 is considered one of the test results which seem to support the use of Rocha's assumptions.

More definite test results which support the applicability of Rocha's assumptions are available for the soil skeleton under drained cyclic loading conditions. During the cyclic loadings, a stress-strain relation usually becomes a hysteresis loop as shown in Fig. 6. The main characteristics of the hysteresis loop are inclination and roundness of the loop. These characteristics are usually expressed by the normalised secant shear modulus G/G_0 and the hysteretic damping factor h ; G/G_0 is defined as the ratio of secant modulus at the reversal stress point against the shear modulus at the strain level of 10^{-6} and h is given by $h = \Delta W / (4\pi W)$ in which ΔW is the area within the hysteresis loop and W is the virtual elastic strain energy as shown in Fig. 6. In general, G/G_0 and h depend on the shear strain amplitude γ (i.e. shear strain at the reversal stress point). Kong, et al. (1986) conducted cyclic torsional shear tests under the confining pressures ranging from 0.05 to 0.84 kgf/cm² (from 5 to 82 kN/m²) and presented the results together with the test results under the confining pressure of 1 kgf/cm² (98 kN/m²) obtained by Tatsuoka et al. (1978). The results indicate, as shown in Fig. 7, that, if the shear strain amplitude is normalised by the scaling factor $\gamma_{0.5}$, which is the shear strain amplitude at $G/G_0 = 0.5$, G/G_0 is uniquely determined irrespective of the confining pressures. The

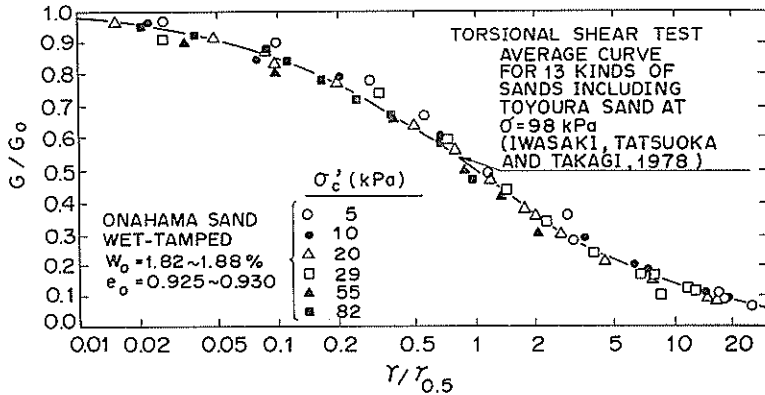


Fig. 7 Normalised secant shear modulus of Onahama and Toyoura sands as a function of normalised shear strain amplitude at the confining pressures ranging from 0.05 to 1 kgf/cm² (from 5 to 98kN/m²) (after Kong, et al, 1986; Tatsuoka, et al, 1978)

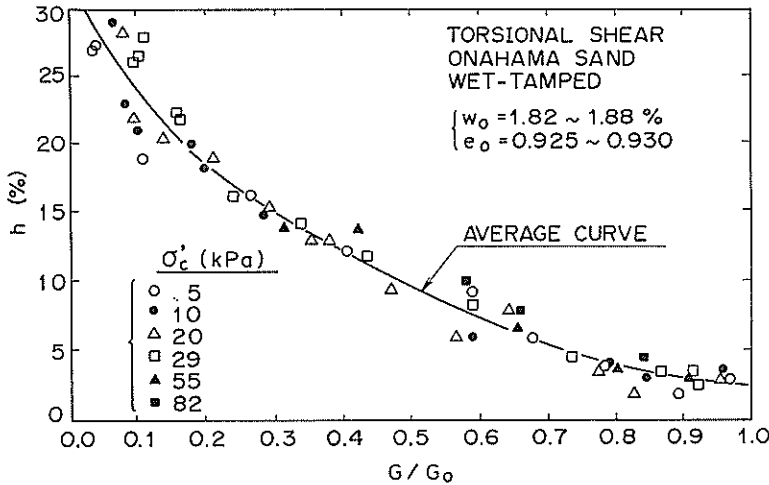


Fig. 8 Hysteretic damping of Onahama sand as a function of normalised secant shear modulus at the confining pressures ranging from 0.05 to 0.84kgf/cm² (from 5 to 82 kN/m²) (after Kong, et al, 1986)

similar conclusion is drawn upon the damping, which is, as mentioned earlier, the measure of the roundness of the hysteresis loop. As shown in Fig. 8, h is uniquely determined from G/G_o , which is, as mentioned earlier, determined irrespective of confining pressures from the normalised shear strain.

Thus, there are several test results which support Rocha's assumptions. Consequently, if the deformation, rather than the ultimate state of stability, is of major concern, Rocha's assumptions are considered applicable.

5. Applicability of the Similitude

In deriving the similitude, the basic equations are considered valid. However,

in deriving the basic equations, the following idealizations or approximations have been adopted; (1) soil skeleton is regarded as continuum, (2) deformation is regarded small so that the equilibrium equation after deformation is the same as that before the deformation, and (3) strain of the soil skeleton is regarded small so that the linear approximation of displacement-strain relation by Eq. (2) holds true. Consequently, there are following limitations in the applicability of the similitude; (1) the similitude is not applicable to the phenomenon at which soil particles completely lose contacts among themselves such as ultimate state of liquefaction, and (2) the similitude is not applicable to the phenomenon at which the deformation or the strain is too large to satisfy the abovementioned approximations.

As mentioned in the previous section, it is usual that the major concern in the shaking table tests of saturated soil-structure-fluid system is the deformation rather than the ultimate state of stability. The degree of the deformation which is useful to study in practice is not so large as to violate the abovementioned limitations; if the degree of the deformation is specified in terms of shear strain levels, it is about 10 percent, in the prototype, at the maximum. Therefore, despite the limitations mentioned above, the similitude obtained in the present study has a fairly wide applicability to such research subjects of practical importance as assessing the degree of deformation of bulkheads due to earthquake loadings, designing the area of ground reinforcement, etc.

6. Similitude Applied to Liquefaction

In the framework presented in Eqs. (1) through (6), liquefaction of saturated sand is nothing but a special case among the general behaviour of the two phase medium; increase of pore water pressure due to plastic volumetric strain. Because the liquefaction of saturated sand plays an important role in the earthquake and geotechnical engineering practice, it may be worth to study some aspect of the similitude derived here when the similitude is applied to the phenomenon of liquefaction.

According to the similitude derive in this study, all the components of the effective stress are unique determined by the scaling factor λ_σ . Thus, the shear stress ratio, i.e. the ratio of the deviatoric stress component over the mean effective stress, is uniquely determined irrespective of the geometric scale of the model.

However, there is one factor which is rather difficult to control in conducting the model tests in accordance with the similitude; the scaling factor for bulk modulus of pore water. In what follows, the influence of the bulk modulus of pore water upon the liquefaction will be considered.

Under the undrained condition, $w=0$. By regarding $1/K_s=0$, Eq. (6) gives

$$p = -(K_t/n)m^T \epsilon \dots\dots\dots(50)$$

in which

- p: pore water pressure
- K_t : bulk modulus of pore water
- n: prosity of the soil
- $m^T = (1, 1, 1, 0, 0, 0)$
- $\epsilon = (\epsilon_{11}, \epsilon_{22}, \epsilon_{33}, \gamma_{12}, \gamma_{23}, \gamma_{31})$: strain

Let us regard the volumetric strain $m^T \epsilon$ as a sum of the elastic and the plastic components;

$$\mathbf{m}^T \boldsymbol{\varepsilon} = (\mathbf{m}^T \boldsymbol{\varepsilon})_{el} + (\mathbf{m}^T \boldsymbol{\varepsilon})_{pl} \quad \dots\dots\dots(51)$$

in which

$(\mathbf{m}^T \boldsymbol{\varepsilon})_{el}$: elastic volumetric strain

$(\mathbf{m}^T \boldsymbol{\varepsilon})_{pl}$: plastic volumetric strain

Let us denote the rebound modulus of soil skeleton as K , i.e. a coefficient of a part of the tangential stiffness matrix \mathbf{D} in Eq. (3) which contributes to the elastic volumetric strain of the skeleton; namely, by regarding $d\boldsymbol{\varepsilon}^0=0$ and $1/K_s=0$, Eq. (3) gives

$$d[(1/3)\mathbf{m}^T \boldsymbol{\sigma}'] = Kd(\mathbf{m}^T \boldsymbol{\varepsilon})_{el} \quad \dots\dots\dots(52)$$

Substituting Eq. (1) into Eq. (52) yields

$$d\sigma_m + dp = Kd(\mathbf{m}^T \boldsymbol{\varepsilon})_{el} \quad \dots\dots\dots(53)$$

in which $\sigma_m = (1/3)\mathbf{m}^T \boldsymbol{\sigma}$: mean total stress

Eliminating the elastic volumetric strain $(\mathbf{m}^T \boldsymbol{\varepsilon})_{el}$ from Eqs. (50) and (53) yields the following relation between the pore water and the plastic volumetric strain;

$$dp = -[1/(1+\alpha)][Kd(\mathbf{m}^T \boldsymbol{\varepsilon})_{pl} + d\sigma_m] \quad \dots\dots\dots(54)$$

in which

$$\alpha = K/(K_t/n)$$

For most of the soils, the term α is close to zero. Therefore, the similitude derived earlier is also applicable for the liquefaction phenomenon even though the bulk modulus of the pore water does not exactly follow the similitude. According to the similitude, as mentioned earlier, the shear stress ratio is uniquely determined irrespective of the geometric scale of the model.

At present, test data are not available to get a convincing conclusion whether the shear stress ratio depends on the confining pressures or not. If the bulk modulus of soil skeleton K (i.e. rebound modulus) does not exactly follow the similitude, pore water pressures will be accordingly affected as understood from Eq. (54). In this case, the similitude is not exactly applicable to the liquefaction. However, even in this case, Eq. (54) suggests that the deviation of pore water pressures from those given by the similitude is proportional to the small deviation of the bulk modulus of soil skeleton from that given by the similitude. Consequently, the similitude derived in this study will give, at least, a good approximation on the behaviour of the prototype which involves the liquefaction phenomenon.

The only reservation is, as mentioned earlier, that the similitude is not applicable to (1) the phenomenon at which soil particles completely lose contacts among themselves, (2) the phenomenon at which the deformation or the strain is too large, and (3) the phenomenon at which ultimate failure of soil is involved. As mentioned earlier, assessment of intermediate deformation of soil structures and foundations is often of the major concern in the earthquake engineering. Therefore, despite the limitations mentioned above, the similitude obtained in the present study has a fairly wide applicability to the phenomena which involve the liquefaction of medium and dense sands such as assessing the deformation of offshore and waterfront structures due to liquefaction of medium and dense sands, designing the area of ground compaction as a countermeasure against liquefaction, etc.

7. Conclusions

A theoretical consideration has been given to the similitude for shaking table tests of saturated soil-structure-fluid systems in the $1g$ gravitational field. The consideration is based on the basic equations which govern the behaviour of the saturated soil-structure-fluid systems under dynamic loadings. As a result, a similitude has been derived.

Applicability of the similitude derived in the present study has been examined by using the presently available test data. The result indicates that the similitude will give a good approximation on the behaviour of the prototype if the deformation of the soil-structures under earthquake loadings are of major concern in the model test.

(Received on June 28, 1988)

References

- 1) DE BEER, E. E. (1965): "The scale effect on the phenomenon of progressive rupture in cohesionless soils," *Proc. 6th I.C.S.M.F.E.*, Vol. II, pp. 13-17.
- 2) KAGAWA, T. (1978): "On the similitude in model vibration tests of earth-structures," *Proc. of Japan Society of Civil Engineers*, No. 275, pp. 69-77 (in Japanese).
- 3) KOKUSHO, T. and IWATATE, T. (1979): "Scaled model tests and numerical analyses on nonlinear dynamic response of soft grounds," *Proc. of Japan Society of Civil Engineers*, No. 285, pp. 57-67 (in Japanese).
- 4) KONG, X. J., TATSUOKA, F. and PRADHAN, T. B. S. (1986): "Dynamic deformation properties of sand at extremely low pressures," *Proc. of 7th Japan Earthquake Engineering Symposium*, pp. 631-636.
- 5) LAMB, H. (1932): "Hydrodynamics," 6th ed. Cambridge.
- 6) PRADHAN, T. B. S., SATO, Y. and TATSUOKA, F. (1987): "Undrained stress-strain relations of sands under earthquake loadings," *19th Jishin Kogaku Kenkyu Happyou Kai (19th Research Conference on Earthquake Engineering)*, Japan Society of Civil Engineers, pp. 213-216 (in Japanese).
- 7) ROCHA, M. (1957): "The possibility of solving soil mechanics problems by the use of models," *Proc. 4th I.C.S.M.F.E.*, Vol. 1, pp. 183-188.
- 8) TATSUOKA, F., IWASAKI, T. and TAKAGI, Y. (1978): "Hysteretic damping of sands under cyclic loading and its relation to shear modulus," *Soils and Foundations*, Vol. 18, No. 2, pp. 25-40.
- 9) TATSUOKA, F., SAKAMOTO, M., KAWAMURA, T., and FUKUSHIMA, S. (1986): "Strength and deformation characteristics of sand in plane strain compression at extremely low pressures," *Soils and Foundations*, Vol. 26, No. 1, pp. 65-84.
- 10) TAYLOR, D. W. (1948): "Fundamentals of Soil Mechanics," John Wiley & Sons.
- 11) YAMAGUCHI, H., KIMURA, T., and FUJI-I, N. (1976): "On the influence of progressive failure on the bearing capacity of shallow foundations in dense sand," *Soils and Foundations*, Vol. 16, No. 4, pp. 11-22.
- 12) ZIENKIEWICZ, O. C., CHANG, C. T. and BETTESS, T. (1980): "Drained undrained, consolidating and dynamic behaviour assumptions in soils. Limits of validity," *Geotechnique*, Vol. 30, No. 4, pp. 385-395.

Notation

- D**: tangent modulus, which is defined by the constitutive law and generally depends on histories of σ' , ϵ , etc.
EA: longitudinal rigidity (per unit breadth of the beam) = Young's modulus \times cross sectional area (per unit breadth of the beam)
EI: flexural rigidity (per unit breadth of the beam) = Young's modulus \times second moment of area (per unit breadth of the beam)
F: axial force specified at the boundary (per unit breadth of the beam)
G: second shear modulus at cyclic shear test
G₀: shear modulus of soil at small strain level
g^T = (0, g, 0): acceleration of gravity (g = 980 Gals)
h: hysteretic damping factor; $h = \Delta W / (4\pi W)$
i: hydraulic gradient specified at the boundary
K: rebound modulus of the soil skeleton
K_t: bulk modulus of the pore water
K_s: average bulk modulus of the solid grains forming the soil skeleton
k: permeability

$$\mathbf{L}^T = \begin{bmatrix} \frac{\partial}{\partial x_1} & 0 & 0 & \frac{\partial}{\partial x_2} & 0 & \frac{\partial}{\partial x_3} \\ 0 & \frac{\partial}{\partial x_2} & 0 & \frac{\partial}{\partial x_1} & \frac{\partial}{\partial x_3} & 0 \\ 0 & 0 & \frac{\partial}{\partial x_3} & 0 & \frac{\partial}{\partial x_2} & \frac{\partial}{\partial x_1} \end{bmatrix}$$

- M**: bending moment specified at the boundary (per unit breadth of the beam)
m^T = (1, 1, 1, 0, 0, 0)
n: porosity of the soil skeleton
n: unit normal vector
p: pore water pressure
 \bar{p} : pore water pressure specified on the boundary
S: a matrix which transforms the stress into the traction on the specified surface
 \bar{S} : shear force specified at the boundary (per unit breadth of the beam)
 \bar{T} : traction specified on the boundary
t: unit tangential vector
u^T = (u₁, u₂, u₃): displacement of soil skeleton and/or beam
 \bar{u} : displacement specified on the boundary
 \ddot{u} : acceleration of soil and/or structure
V_s: shear wave velocity
W: virtual elastic strain energy at cyclic shear test
 ΔW : area within the hysteresis loop at cyclic shear test
w^T = (w₁, w₂, w₃): average displacement of pore water relative to the soil skeleton;
 i.e. the ratio of the quantity of the pore water displaced over the total cross-sectional area
 \bar{w} : relative displacement of pore water specified on the boundary
x^T = (x₁, x₂, x₃): cartesian coordinate
 $\nabla^T = \left(\frac{\partial}{\partial x_1}, \frac{\partial}{\partial x_2}, \frac{\partial}{\partial x_3} \right)$

- $\alpha = K / (K_t / n)$
 $\mathbf{e}^T = (\epsilon_{11}, \epsilon_{22}, \epsilon_{33}, \gamma_{12}, \gamma_{23}, \gamma_{31})$: strain
 \mathbf{e}^0 : strain of soil skeleton due to creep, temperature, etc.
 $(\mathbf{m}^T \mathbf{e})_{el}$: elastic volumetric strain
 $(\mathbf{m}^T \mathbf{e})_{pl}$: plastic volumetric strain
 λ : geometric scaling factor
 λ_t : scaling factor for time, strain, etc.
 ρ : apparent density of two phase medium composed of soil and pore water; i.e. density of saturated soil
 ρ_f : density of pore water
 ρ_b : density of the beam (mass per unit length and breadth of the beam)
 Γ_0 , etc.: boundary at which the value of \bar{u} , etc. is specified
 $\bar{\theta}$: inclination of the beam specified at the boundary
 $\boldsymbol{\sigma}^T = (\sigma_{11}, \sigma_{22}, \sigma_{33}, \tau_{12}, \tau_{23}, \tau_{31})$: total stress
 $\boldsymbol{\sigma}^T = (\sigma_{11}, \sigma_{22}, \sigma_{33}, \tau_{12}, \tau_{23}, \tau_{31})$: effective stress
 $\sigma_m = (1/3) \mathbf{m}^T \boldsymbol{\sigma}$: mean total stress
subscripts ()_m and ()_p: model and prototype